Progress In Electromagnetics Research, PIER 40, 113–129, 2003

ELECTROMAGNETIC SCATTERING FROM A DIELECTRIC CYLINDER WITH MULTIPLE ECCENTRIC CYLINDRICAL INCLUSIONS

H. Toyama, K. Yasumoto, and T. Iwasaki

Department of Computer Science and Communication Engineering
Kyushu University 36
Fukuoka 812-8581, Japan

Abstract—A simple and direct method to the problem of two-dimensional electromagnetic scattering from a dielectric cylinder with multiple eccentric cylindrical inclusions is proposed. The method is based on the T-matrix approach. An aggregate T-matrix of the external cylinder for TM-wave and TE-wave excitations is derived in terms of the T-matrices of individual cylinders isolated in the host medium. The backscattering and differential scattering cross-sections of the host cylinder are easily obtained by matrix calculations for the aggregate T-matrix. Numerical investigation is presented for the case where all cylinders have circular cross-sections. Numerical examples for up to three inclusions demonstrate that the scattering characteristics are significantly influenced by the internal asymmetry and inhomogeneity pertinent to the locations and material of the inclusions.

1. INTRODUCTION

Electromagnetic wave scattering from concentrically stratified or eccentrically stratified cylinders has been considerable theoretical interest over the years [1–5]. When cylindrical structures are embedded into a dielectric cylinder, there occur multiple scatterings of interior fields between the cylindrical inclusions and the outer boundary of the host cylinder. The far-field scattering exhibits different characteristics from those by a homogeneous dielectric cylinder. This feature has many practical applications such as simulation of complex scattering structures, detection of the internal inhomogeneity of cylindrical objects, and control of the scattering cross-section of a dielectric cylinder. Recently, Stratigaki et al. [6] have reported a rigorous solution to the problem of two-dimensional plane-wave scattering from a circular dielectric cylinder with N-parallel cylindrical dielectric inclusions of circular cross-sections by using the indirect mode-matching formulation.

In this paper, we shall present a simple and direct method for the problem of two-dimensional scattering from a dielectric cylinder with multiple cylindrical inclusions, using the T-matrix formulation [7] for a single cylindrical scatterer and the recursive T-matrix algorithm [8] for multiple cylindrical scatterers. In this approach, the T-matrix is first defined for individual cylindrical inclusions isolated in the host medium of infinite extent. The results are substituted into a recursive algorithm to derive the T-matrix of each cylinder in the presence of multiple cylinders. The T-matrix of each cylinder are transformed into the coordinate with the origin at the center of the host cylinder and combined. Then the scattered fields inside the host cylinder are expressed in terms of a single T-matrix. Applying the boundary conditions at the outer surface of the host cylinder to the internal and external scattered fields, the aggregate T-matrix of the composite cylindrical system is finally obtained for TM-wave and TE-wave excitations. The approach is straightforward and quite general. The cylindrical inclusions may be dielectric, air hole, perfect conductor, or their mixture with different dimensions. If all cylinders have circular cross-sections, the aggregate T-matrix is given in closed form. The scattering characteristics of the host cylinder can be obtained by simpler matrix calculations for the aggregate T-matrix with a suitable truncation of matrix size.

Numerical investigation is presented for the case where all cylinders have circular cross-sections. The result validates that the proposed method yields concise exact solutions. If the truncation size of the aggregate T-matrix is large enough, the solutions obtained for

two inclusions satisfy the optical theorem and reciprocity relation with the errors less than 10^{-14}. The numerical examples of backscattering, forward scattering and differential scattering cross-sections for up to three inclusions demonstrate that the scattering characteristics have a close link to the internal asymmetry and inhomogeneity pertinent to the locations and material of inclusions.

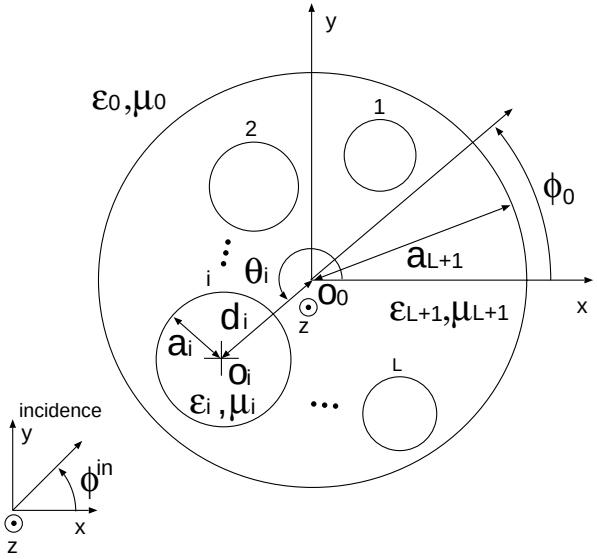

Figure 1. Cross-section of a dielectric cylinder with L parallel cylindrical inclusions.

2. FORMULATION OF THE PROBLEM

The geometry discussed here is shown in Fig. 1. The L circular cylinders of radius $a_1, a_2, \cdots, a_L$ are included in a dielectric circular cylinder of radius a_{L+1}. The cylinders are infinitely long along z axis and parallel to each other. The permittivity and permeability of each cylindrical region are denoted by ε_i and μ_i $(i = 1, 2, \cdots, L, L+1)$, and the exterior of the host cylinder is free space with ε_0 and μ_0. The origin O_0 of the global coordinate xOy is attached to the center of the host cylinder and the origin O_i of i-th cylindrical inclusions are centered at (d_i, θ_i) where d_i is the distance from the global origin O_0 and θ_i is the polar angle measured from Ox axis. The global polar coordinate in xOy is denoted by $\boldsymbol{r}_0 = (\rho_0, \phi_0)$, whereas the local polar coordinate attached to each cylindrical inclusion is by $\boldsymbol{r}_i = (\rho_i, \phi_i)$

$(i = 1, 2, \cdots, L)$. We consider the scattering of a plane electromagnetic wave which is incident in the direction normal to the cylinder axis. The problem is then reduced to a two-dimensional one and may be treated separately for TM and TE waves relative to the z axis.

Let $\psi(\boldsymbol{r})$ be the E_z field for TM wave and the H_z field for TE wave. The scattered field $\psi^{sc}_{L+1}(\boldsymbol{r})$ in the interior of the host medium assigned the number $L+1$ is expressed as follows:

$$\psi^{sc}_{L+1}(\boldsymbol{r}) = \sum_{n=-\infty}^{\infty} b_n J_n(k_{L+1}\rho_0)e^{in\phi_0} + \sum_{i=1}^{L}\left[\sum_{m=-\infty}^{\infty} c_{i,m} H^{(1)}_m(k_{L+1}\rho_i)e^{im\phi_i}\right] \tag{1}$$

where $k_{L+1} = \omega\sqrt{\varepsilon_{L+1}\mu_{L+1}}$, J_n is the n-th order Bessel function, $H^{(1)}_m$ is the m-th order Hankel function of the first kind, and b_n and $c_{i,m}$ are unknown amplitudes of the scattered fields expressed in terms of cylindrical harmonic expansions. The second term in Eq. (1) comprises the diverging cylindrical waves from each of L cylindrical inclusions assigned $i = 1, 2, \cdots, L$, and the first term represents the field scattered from the outer boundary $\rho_0 = a_{L+1}$ of the host cylinder which behaves like an incident field on the L inclusions. To discriminate the difference in scattering origins, we have used the index n for the expansion relative to the global origin O_0 and the index m for the expansions relative to each local origin O_i. Equation (1) is written in a vectorial form as

$$\psi^{sc}_{L+1}(\boldsymbol{r}) = \boldsymbol{\Phi}^T_{L+1}(\boldsymbol{r}_0)\cdot\boldsymbol{B} + \sum_{i=1}^{L}\boldsymbol{\Psi}^T_{L+1}(\boldsymbol{r}_i)\cdot\boldsymbol{C}_i \tag{2}$$

with

$$\boldsymbol{\Phi}_{L+1}(\boldsymbol{r}_0) = [J_n(k_{L+1}\rho_0)e^{in\phi_0}] \tag{3}$$

$$\boldsymbol{\Psi}_{L+1}(\boldsymbol{r}_i) = [H^{(1)}_m(k_{L+1}\rho_i)e^{im\phi_i}] \tag{4}$$

$$\boldsymbol{B} = [b_n], \quad \boldsymbol{C}_i = [c_{i,m}] \tag{5}$$

where the vector quantities are defined as column vectors and the superscript T indicates the transpose of vectors.

Although $\boldsymbol{B}$ is unknown, the right hand side of Eq. (2) can be viewed as the total field external to the L cylinders in the presence of an incident field $\boldsymbol{\Phi}^T_{L+1}(\boldsymbol{r}_0)\cdot\boldsymbol{B}$. Using the translational formulas of cylindrical harmonics between the global coordinate and each of local coordinates and the T-matrix algorithm [8], the amplitude vectors $\boldsymbol{C}_i$ can be expressed in terms of $\boldsymbol{B}$ and Eq. (2) is rewritten as follows:

$$\boldsymbol{\psi}^{sc}_{L+1}(\boldsymbol{r}_0) = [\boldsymbol{\Phi}^T_{L+1}(\boldsymbol{r}_0) + \boldsymbol{\Psi}^T_{L+1}(\boldsymbol{r}_0)\cdot\bar{\bar{\boldsymbol{T}}}_L]\cdot\boldsymbol{B} \tag{6}$$

with

$$\bar{\bar{\boldsymbol{T}}}_L = \sum_{i=1}^{L} \bar{\bar{\boldsymbol{\beta}}}_{0,i} \cdot \bar{\bar{\boldsymbol{T}}}_{i(L)} \cdot \bar{\bar{\boldsymbol{\beta}}}_{i,0} \tag{7}$$

$$\boldsymbol{\Psi}_{L+1}(\boldsymbol{r}_0) = [H_n^{(1)}(k_{L+1}\rho_0)e^{in\phi_0}] \tag{8}$$

where $\bar{\bar{\boldsymbol{T}}}_L$ represents an aggregate T-matrix for the L cylinders viewed from the global origin O_0, $\bar{\bar{\boldsymbol{T}}}_{i(L)}$ is the T-matrix for the i-th cylinder in the presence of L cylinders in the host medium of infinite extent, and $\bar{\bar{\boldsymbol{\beta}}}_{i,j}$ is the translation matrix [8] for the regular part of cylindrical harmonics between the i and j coordinates. The T-matrix $\bar{\bar{\boldsymbol{T}}}_{i(L)}$ is calculated using the recursive algorithm [8] for L scatterers as follows:

$$\bar{\bar{\boldsymbol{T}}}_{\ell+1(\ell+1)} \cdot \bar{\bar{\boldsymbol{\beta}}}_{\ell+1,0} = [\bar{\bar{\boldsymbol{I}}} - \bar{\bar{\boldsymbol{T}}}_{\ell+1(1)} \cdot \sum_{i=1}^{\ell} \bar{\bar{\boldsymbol{\alpha}}}_{\ell+1,i} \cdot \bar{\bar{\boldsymbol{T}}}_{i(\ell)} \cdot \bar{\bar{\boldsymbol{\beta}}}_{i,0} \cdot \bar{\bar{\boldsymbol{\beta}}}_{0,i} \cdot \bar{\bar{\boldsymbol{\alpha}}}_{i,\ell+1}]^{-1}$$

$$\times \bar{\bar{\boldsymbol{T}}}_{\ell+1(1)} \cdot [\bar{\bar{\boldsymbol{\beta}}}_{\ell+1,0} + \sum_{i=1}^{\ell} \bar{\bar{\boldsymbol{\alpha}}}_{\ell+1,i} \cdot \bar{\bar{\boldsymbol{T}}}_{i(\ell)} \cdot \bar{\bar{\boldsymbol{\beta}}}_{i,0}] \tag{9}$$

$$\bar{\bar{\boldsymbol{T}}}_{i(\ell+1)} \cdot \bar{\bar{\boldsymbol{\beta}}}_{i,0} = \bar{\bar{\boldsymbol{T}}}_{i(\ell)} \cdot \bar{\bar{\boldsymbol{\beta}}}_{i,0} + \bar{\bar{\boldsymbol{T}}}_{i(\ell)} \cdot \bar{\bar{\boldsymbol{\beta}}}_{i,0} \cdot \bar{\bar{\boldsymbol{\beta}}}_{0,i} \cdot \bar{\bar{\boldsymbol{\alpha}}}_{i,\ell+1} \cdot \bar{\bar{\boldsymbol{T}}}_{\ell+1(\ell+1)} \cdot \bar{\bar{\boldsymbol{\beta}}}_{\ell+1,0} \tag{10}$$

where $\ell = 1, 2, \cdots, L-1$, $i = 1, 2, \cdots, \ell$, $\boldsymbol{I}$ is the unit matrix, and $\bar{\bar{\boldsymbol{\alpha}}}_{i,j}$, is the translation matrices [8, 9] for cylindrical harmonics between the i and j coordinate systems, and has been used the identity

$$\bar{\bar{\boldsymbol{\beta}}}_{i,0} \cdot \bar{\bar{\boldsymbol{\beta}}}_{0,i} = \bar{\bar{\boldsymbol{I}}}. \tag{11}$$

The recursion using Eqs. (9) and (10) starts with the individual T-matrices $\bar{\bar{\boldsymbol{T}}}_{i(1)}$ for the isolated ith circular cylinder in the host medium of infinite extent.

When a circular cylinder of radius a_i, permittivity ε_i, and permeability μ_i is located in a background medium with permittivity ε_{L+1} and permeability μ_{L+1}, the T-matrix of the cylinder is given by the following diagonal matrix:

$$\begin{aligned} \bar{\bar{\boldsymbol{T}}}_{i(1)} &= -[\eta_{L+1}\bar{\bar{\boldsymbol{H}}}'_{L+1,i} - \eta_i \bar{\bar{\boldsymbol{J}}}'_{i,i} \cdot \bar{\bar{\boldsymbol{J}}}_{i,i}^{-1} \cdot \bar{\bar{\boldsymbol{H}}}_{L+1,i}]^{-1} \\ &\quad \times [\eta_{L+1}\bar{\bar{\boldsymbol{J}}}'_{L+1,i} - \eta_i \bar{\bar{\boldsymbol{J}}}'_{i,i} \cdot \bar{\bar{\boldsymbol{J}}}_{i,i}^{-1} \cdot \bar{\bar{\boldsymbol{J}}}_{L+1,i}] \quad \text{for TM wave} \end{aligned} \tag{12}$$

$$\begin{aligned} \bar{\bar{\boldsymbol{T}}}_{i(1)} &= -[\eta_i \bar{\bar{\boldsymbol{H}}}'_{L+1,i} - \eta_{L+1}\bar{\bar{\boldsymbol{J}}}'_{i,i} \cdot \bar{\bar{\boldsymbol{J}}}_{i,i}^{-1} \cdot \bar{\bar{\boldsymbol{H}}}_{L+1,i}]^{-1} \\ &\quad \times [\eta_i \bar{\bar{\boldsymbol{J}}}'_{L+1,i} - \eta_{L+1}\bar{\bar{\boldsymbol{J}}}'_{i,i} \cdot \bar{\bar{\boldsymbol{J}}}_{i,i}^{-1} \cdot \bar{\bar{\boldsymbol{J}}}_{L+1,i}] \quad \text{for TE wave} \end{aligned} \tag{13}$$

with

$$\bar{\bar{\boldsymbol{J}}}_{i,i} = [J_m(k_i a_i)\delta_{m,m'}],\ \bar{\bar{\boldsymbol{J}}}'_{i,i} = [J'_m(k_i a_i)\delta_{m,m'}]\ (i = 1, 2, 3, \cdots, L) \quad (14)$$

$$\bar{\bar{\boldsymbol{J}}}_{L+1,i} = [J_m(k_{L+1} a_i)\delta_{m,m'}], \quad \bar{\bar{\boldsymbol{J}}}'_{L+1,i} = [J'_m(k_{L+1} a_i)\delta_{m,m'}] \quad (15)$$

$$\bar{\bar{\boldsymbol{H}}}_{L+1,i} = [H^{(1)}_m(k_{L+1} a_i)\delta_{m,m'}], \quad \bar{\bar{\boldsymbol{H}}}'_{L+1,i} = [H^{(1)'}_m(k_{L+1} a_i)\delta_{m,m'}] \quad (16)$$

$$k_i = \omega\sqrt{\varepsilon_i \mu_i}, \quad k_{L+1} = \omega\sqrt{\varepsilon_{L+1}\mu_{L+1}},$$
$$\eta_i = \sqrt{\varepsilon_i/\mu_i}, \quad \eta_{L+1} = \sqrt{\varepsilon_{L+1}/\mu_{L+1}} \quad (17)$$

where $\delta_{m,m'}$ is the Kronecker's delta, and the prime on the Bessel and Hankel functions denotes their derivatives with respect to the indicated arguments. The T-matrix for a cylinder of perfect conductor is easily deduced by taking the limit $|\varepsilon_i| \to \infty$ in Eqs. (12) and (13). Using Eqs. (9)–(13) in Eq. (7), the solution to the scattered field $\psi^{sc}_{L+1}(\boldsymbol{r}_0)$ in the interior of the host medium is completed for both TM and TE waves except for the unknown amplitude vector $\boldsymbol{B}$.

When a plane wave of unit amplitude is incident on the host cylinder with an angle ϕ^{in} measured from the Ox axis, the total field in the exterior of the host cylinder is expressed in terms of the global polar coordinate as follows:

$$\begin{aligned} \psi_0(\boldsymbol{r}_0) &= \psi^{in}_0(\boldsymbol{r}_0) + \psi^{sc}_0(\boldsymbol{r}_0) \\ &= \boldsymbol{\Phi}^T_0(\boldsymbol{r}_0) \cdot \boldsymbol{A}^{in} + \boldsymbol{\Psi}^T_0(\boldsymbol{r}_0) \cdot \boldsymbol{A}^{sc} \end{aligned} \quad (18)$$

with

$$\boldsymbol{\Phi}_0(\boldsymbol{r}_0) = [J_n(k_0\rho_0)e^{in\phi_0}] \quad (19)$$

$$\boldsymbol{\Psi}_0(\boldsymbol{r}_0) = [H^{(1)}_n(k_0\rho_0)e^{in\phi_0}] \quad (20)$$

$$\boldsymbol{A}^{in} = [(i)^n e^{-in\phi^{in}}] \quad (21)$$

$$\boldsymbol{A}^{sc} = [a^{sc}_n] \quad (22)$$

where $\boldsymbol{A}^{in}$ is the known incident amplitude vector and $\boldsymbol{A}^{sc}$ is the unknown amplitude vector for the scattered field in the exterior of the host cylinder. The tangential field components derived from Eq. (6) in the interior region and from Eq. (18) in the exterior region must be continuous across the outer boundary $\rho_0 = a_{L+1}$ of the host cylinder. Applying the boundary conditions, the unknown amplitude vectors $\boldsymbol{B}$ and $\boldsymbol{A}^{sc}$ are related to the amplitude vector $\boldsymbol{A}^{in}$ of the incident wave. After several manipulations, the scattered field $\psi^{sc}_0(\boldsymbol{r}_0)$ in the exterior region can be finally determined as

$$\psi^{sc}_0(\boldsymbol{r}_0) = \boldsymbol{\Psi}^T_0(\boldsymbol{r}_0) \cdot \bar{\bar{\boldsymbol{T}}}_{L+1} \cdot \boldsymbol{A}^{in} \quad (23)$$

with

$$\bar{\bar{\boldsymbol{T}}}_{L+1} = -[\eta_0 \bar{\bar{\boldsymbol{H}}}'_{0,L+1} - \eta_{L+1} \bar{\bar{\boldsymbol{F}}}'_{L+1,L+1} \cdot \bar{\bar{\boldsymbol{F}}}^{-1}_{L+1,L+1} \cdot \bar{\bar{\boldsymbol{H}}}_{0,L+1}]^{-1} \times [\eta_0 \bar{\bar{\boldsymbol{J}}}'_{0,L+1} - \eta_{L+1} \bar{\bar{\boldsymbol{F}}}'_{L+1,L+1} \cdot \bar{\bar{\boldsymbol{F}}}^{-1}_{L+1,L+1} \cdot \bar{\bar{\boldsymbol{J}}}_{0,L+1}] \quad \text{for TM wave} \tag{24}$$

$$\bar{\bar{\boldsymbol{T}}}_{L+1} = -[\eta_{L+1} \bar{\bar{\boldsymbol{H}}}'_{0,L+1} - \eta_0 \bar{\bar{\boldsymbol{F}}}'_{L+1,L+1} \cdot \bar{\bar{\boldsymbol{F}}}^{-1}_{L+1,L+1} \cdot \bar{\bar{\boldsymbol{H}}}_{0,L+1}]^{-1} \times [\eta_{L+1} \bar{\bar{\boldsymbol{J}}}'_{0,L+1} - \eta_0 \bar{\bar{\boldsymbol{F}}}'_{L+1,L+1} \cdot \bar{\bar{\boldsymbol{F}}}^{-1}_{L+1,L+1} \cdot \bar{\bar{\boldsymbol{J}}}_{0,L+1}] \quad \text{for TE wave} \tag{25}$$

$$\bar{\bar{\boldsymbol{F}}}_{L+1,L+1} = \bar{\bar{\boldsymbol{J}}}_{L+1,L+1} + \bar{\bar{\boldsymbol{H}}}_{L+1,L+1} \cdot \bar{\bar{\boldsymbol{T}}}_L \tag{26}$$

$$\bar{\bar{\boldsymbol{F}}}'_{L+1,L+1} = \bar{\bar{\boldsymbol{J}}}'_{L+1,L+1} + \bar{\bar{\boldsymbol{H}}}'_{L+1,L+1} \cdot \bar{\bar{\boldsymbol{T}}}_L \tag{27}$$

where $\bar{\bar{\boldsymbol{T}}}_{L+1}$ denotes an aggregate T-matrix of the host cylinder with L cylindrical inclusions, the matrix $\bar{\bar{\boldsymbol{T}}}_L$ is given by Eq. (7), and the matrices $\bar{\bar{\boldsymbol{J}}}_{j,i}$, $\bar{\bar{\boldsymbol{J}}}'_{j,i}$, $\bar{\bar{\boldsymbol{H}}}_{j,i}$, and $\bar{\bar{\boldsymbol{H}}}'_{j,i}$ are defined by Eqs. (14)–(16). Note that $\bar{\bar{\boldsymbol{T}}}_L = 0$ in the absence of L cylindrical inclusions. In this case, the aggregate T-matrix $\bar{\bar{\boldsymbol{T}}}_{L+1}$ given by Eqs. (24) and (25) reduces to the conventional T-matrix for a homogeneous circular cylinder of radius a_{L+1} occupied by the host medium with ε_{L+1} and μ_{L+1}. The additional terms $\bar{\bar{\boldsymbol{H}}}_{L+1,L+1} \cdot \bar{\bar{\boldsymbol{T}}}_L$ and $\bar{\bar{\boldsymbol{H}}}'_{L+1,L+1} \cdot \bar{\bar{\boldsymbol{T}}}_L$ in Eqs. (26) and (27) explain the influence of the multiple scattering of internal fields under the presence of L cylindrical inclusions.

Although the vectors $\boldsymbol{\Phi}_i(\boldsymbol{r}_j)$, $\boldsymbol{\Psi}_i(\boldsymbol{r}_j)$ and the matrices $\bar{\bar{\boldsymbol{\alpha}}}_{i,j}$, $\bar{\bar{\boldsymbol{\beta}}}_{i,j}$ are of infinite dimensions, the T-matrix algorithm truncate those vectors and matrices with finite dimension. We assume that the sum over n is truncated by $|n| \le N$ and the sum over m is truncated by $|m| \le M$. N represents the number of cylindrical harmonics used to expand the fields at the global origin O_0, whereas M represents the number of harmonics used to expand the fields in each local coordinate system of cylindrical inclusions. When the above truncation is introduced, $\bar{\bar{\boldsymbol{\beta}}}_{i,0}$ is a $(2M+1) \times (2N+1)$ matrix, $\bar{\bar{\boldsymbol{\beta}}}_{0,i}$ is a $(2N+1) \times (2M+1)$ matrix, $\bar{\bar{\boldsymbol{\alpha}}}_{i,j}$ and $\bar{\bar{\boldsymbol{T}}}_{i(\ell)}$ are square matrices with $(2M+1) \times (2M+1)$, and $\bar{\bar{\boldsymbol{T}}}_L$ and $\bar{\bar{\boldsymbol{T}}}_{L+1}$ are square matrices with $(2N+1) \times (2N+1)$.

For the system of circular cylinders, the calculation of $\bar{\bar{\boldsymbol{T}}}_{L+1}$ is straightforward. When $k_0\rho_0 \gg 1$, from Eqs. (20) and (23) we have

$$\psi_0^{sc}(\boldsymbol{r}_0) = \frac{e^{ik_0\rho_0}}{\sqrt{\rho_0}} f(\phi_0, \phi^{in}) \tag{28}$$

with

$$f(\phi_0, \phi^{in}) = \frac{1-i}{\sqrt{\pi k_0}} \sum_{n=-N}^{N} \sum_{n'=-N}^{N} (-i)^n (i)^{n'} e^{i(n\phi_0 - n'\phi^{in})} t_{L+1,nn'} \quad (29)$$

where $t_{L+1,nn'}$ represents the element of n-th row and n'-th column of the aggregate T-matrix $\bar{\bar{\boldsymbol{T}}}_{L+1}$. The differential scattering cross-section $\sigma_d(\phi_0, \phi^{in})$ and the back-scattering cross-section $\sigma_b(\phi^{in} + \pi, \phi^{in})$ per unit length of the host cylinder is obtained as follows:

$$\sigma_d(\phi_0, \phi^{in}) = 2\pi |f(\phi_0, \phi^{in})|^2 \quad (30)$$

$$\sigma_b(\phi^{in}) = 2\pi |f(\phi^{in} + \pi, \phi^{in})|^2. \quad (31)$$

If the host cylinder and L inclusions consist of isotropic and lossless material, the scattered field must satisfy the reciprocity relation and the optical theorem which require, respectively

$$\sigma_d(\phi_0, \phi^{in}) = \sigma_d(\phi^{in} + \pi, \phi_0 + \pi) \quad (32)$$

$$\sigma_t = \frac{4}{k_0} \sum_{n=-N}^{N} | \sum_{n'=-N}^{N} (i)^{n'} e^{-in'\phi^{in}} t_{L+1,nn'} |^2 = -\frac{4}{k_0} \mathrm{Re}\{f(\phi^{in}, \phi^{in})\} \quad (33)$$

where σ_t denotes the total scattering cross-section per unit length of the host cylinder. Equations (32) and (33) can be used to check the accuracy of the solutions.

3. NUMERICAL EXAMPLES

The proposed method has been used to analyze the scattering of electromagnetic plane-wave from a circular dielectric cylinder with inclusions of circular cross-sections under various configurations. All pertinent numerical results shown in [6] were reproduced by our computer code using the aggregate T-matrix. Although a substantial number of numerical examples could be generated, we shall discuss here the results for a host cylinder with up to three inclusions. The truncation numbers M and N in the cylindrical harmonic expansions should be large enough to have a convergent solution [10]. The number M is related to the cross-sectional size of each cylinder and the number N depends on the distance from the center of each cylindrical inclusion to the center of the host cylinder. Testing the convergence of solutions, the numerical examples in what follow wer obtained by choosing $M = N = 12$. The larger truncation numbers are requested when the size of cylindrical inclusions and the host cylinder are further

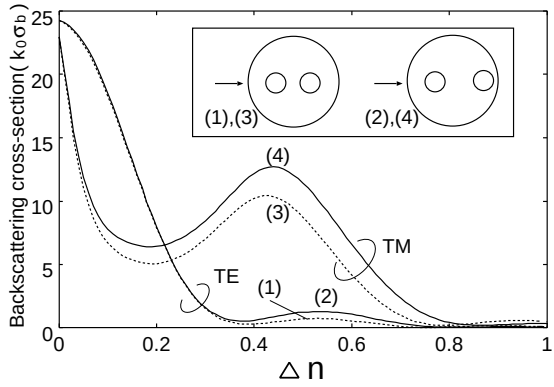

Figure 2. Backscattering cross-section $k_0\sigma_b$ of cylinder with two identical inclusions as functions of the refractive index difference $\Delta n = n_1 - n_3$, where $k_0a_1 = k_0a_2 = 0.25$, $n_1 = n_2 = 2.0$, $k_0d_2 = 1.5$, $\theta_1 = 0°$, $\theta_2 = 180°$, $k_0a_3 = 3.0$, and $\phi^{in} = 0°$. TE wave: (1) $k_0d_1 = 1.5$, (2) $k_0d_1 = 2.25$. TM wave: (3) $k_0d_1 = 1.5$, (4) $k_0d_1 = 2.25$.

increased. The permeability is assumed to be μ_0 over all regions and the refractive index of i-th cylindrical region is denoted by $n_i = \sqrt{\varepsilon_i/\varepsilon_0}$.

We first tested the reciprocity relation and the optical theorem for our solutions. When the number of the inclusions is two, we have seen that both the reciprocity theorem and the optical theorem are rigorously satisfied with the error less than 10^{-14}. The parameters used in those tests are $k_0a_1 = 0.1$, $k_0a_2 = 0.2$, $n_1 = 1.5$, $n_2 = 1.8$, $k_0d_1 = 1.0$, $k_0d_2 = 0.8$, $\theta_1 = 0°$, $k_0a_3 = 2.0$, and $n_3 = 2.0$. The normalized backscattering cross-section $k_0\sigma_b$ for a host cylinder with two inclusions are plotted in Fig. 2 for TM-wave and TE-wave excitations as functions of the refractive index difference $\Delta n = n_1 - n_3$. Two identical dielectric inclusions with $k_0a_1 = k_0a_2 = 0.25$ and $n_1 = n_2 = 2.0$ are placed symmetrically or asymmetrically relative to the center of the host cylinder with $k_0a_3 = 3.0$ and n_3. The direction of incidence of plane wave is $\phi^{in} = 0°$ along the line through the centers of two inclusions. The extreme $\Delta n = 0$ corresponds to a homogeneous cylinder with $k_0a_3 = 3.0$ and $n_3 = 2.0$, whereas the extreme $\Delta n = 1.0$ corresponds to two identical free-standing cylinders. It is seen that the effect of a radial asymmetry is more pronounced for the TM wave excitation. Figure 3 shows the normalized backscattering cross-section $k_0\sigma_b$ of a host cylinder with three inclusions for TM-wave excitation as functions of the position of cylinder 1. Three identical dielectric cylinders with $k_0a_1 = k_0a_2 = k_0a_3 = 0.25$ and $n_1 = n_2 = n_3 = 2.0$ are placed in the host cylinder with $k_0a_4 = 3.0$ and $n_4 = 1.5$. The cylinders 2 and 3

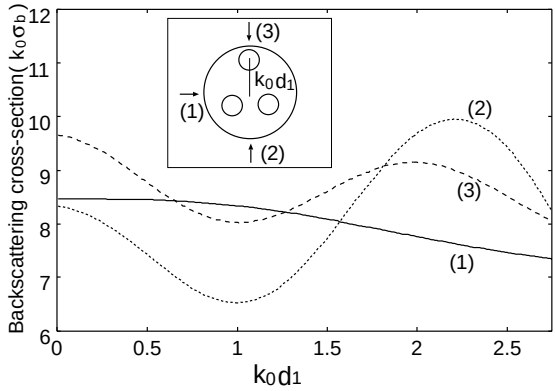

Figure 3. Backscattering cross-section $k_0\sigma_b$ of cylinder with three identical inclusions for TM-wave excitation as functions of the radial position k_0d_1 of cylinder 1, where $k_0a_1 = k_0a_2 = k_0a_3 = 0.25$, $n_1 = n_2 = n_3 = 2.0$, $k_0d_2 = k_0d_3 = 1.5$, $\theta_1 = 90°$, $\theta_2 = 210°$, $\theta_3 = 330°$, $k_0a_4 = 3.0$, and $n_4 = 1.5$. (1) $\phi^{in} = 0°$, (2) $\phi^{in} = 90°$, and (3) $\phi^{in} = 270°$.

are maintained at fixed positions $k_0d_2 = k_0d_3 = 1.5$, $\theta_2 = 210°$, and $\theta_3 = 330°$, whereas the cylinder 1 is assumed to change the position k_0d_1 in the radial direction at $\theta_1 = 90°$. When $k_0d_1 = 1.5$, three inclusions are placed symmetrically relative to the center of the host cylinder. Three different directions of incidence at $\phi^{in} = 0°$, $90°$, and $270°$ are considered. We can see that the backscattering for the incidence at $\phi^{in} = 90°$ is most sensitive to the internal asymmetries. The same cylindrical configurations as shown in Figs. 2 and 3 have been treated in [6] by using the indirect mode-matching method. Our present numerical results are practically identical to those given in Figs. 4 and 8 of [6].

The effect of internally asymmetric scatterers is more pronounced, in general, as the refractive index difference between inclusions and host medium is increased or the size of inclusions relative to the host cylinder is increased. In Fig. 4, the normalized backscattering cross-section $k_0\sigma_b$ and forward scattering cross-section $k_0\sigma_f$ of a host cylinder with a single inclusion and two inclusions are plotted for TM-wave excitation as functions of the incident angle ϕ^{in}. Two identical dielectric cylinders with $k_0a_1 = k_0a_2 = 0.5$ and $n_1 = n_2 = 4.0$ are placed asymmetrically relative to the center of the host cylinder with $k_0a_3 = 2.5$ and $n_3 = 2.0$, where the centers of two cylinders are located at $\theta_1 = 0°$, $\theta_2 = 180°$, $k_0d_1 = 1.5$, and $k_0d_2 = 1.0$. The results obtained with $n_2 = 2.0$ or $n_1 = n_2 = 2.0$ corresponds to the

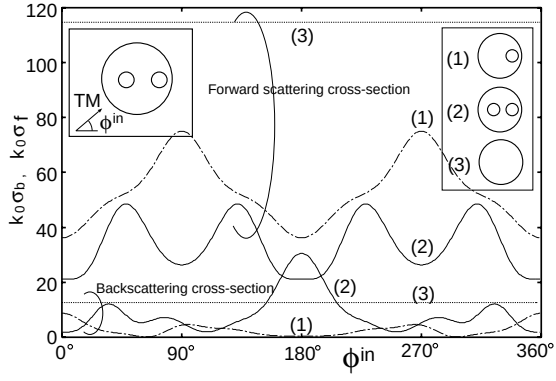

Figure 4. Backscattering cross-section $k_0\sigma_b$ and forward scattering cross-section $k_0\sigma_f$ of cylinder with a single dielectric inclusion or two dielectric inclusions for TM-wave excitation as functions of incident angle ϕ^{in}, where $k_0a_1 = k_0a_2 = 0.5$, $k_0d_1 = 1.5$, $k_0d_2 = 1.0$, $\theta_1 = 0°$, $\theta_2 = 180°$, $k_0a_3 = 2.5$, and $n_3 = 2.0$. (1) a single inclusion: $n_1 = 4.0$ and $n_2 = 2.0$, (2) two inclusions: $n_1 = n_2 = 4.0$, and (3) without inclusions: $n_1 = n_2 = 2.0$.

host cylinder with the single inclusion 1 or a homogeneous cylinder of radius a_3, respectively. The similar plots for TE-wave excitation are shown in Fig. 5. The TM-wave excitation is very sensitive to the internal scatterers. The backscattering cross-section for the host cylinder with two inclusions are greatly enhanced around the incident angle $\phi^{in} = 180°$, whereas the forward scattering cross-section is strongly suppressed around the same incident angle, compared with the case of homogeneous host cylinder. The TE-wave excitation is less sensitive to the internal scatterers, though the backscattering and forward scattering cross-sections change with the incident angle in the presence of geometrical asymmetries. A host cylinder with inclusions of perfect conductor may be regarded as an extreme in the refractive index difference between the host medium and internal scatterers. The normalized backscattering cross-sections $k_0\sigma_b$ and forward scattering cross-section $k_0\sigma_f$ for such a case are treated in Figs. 6 and 7 for TM-wave excitation and TE-wave excitation, respectively. The values of geometrical parameters are same as those given in Figs. 4 and 5 except that the internal cylinders 1 and 2 are perfect conductor with $|n_1| = |n_2| \to \infty$. In this case both TM-wave and TE-wave excitations become very sensitive to the internal asymmetries of scatterers. The backscattering and forward scattering cross-sections of the host cylinder with the single inclusion or two inclusions noticeably

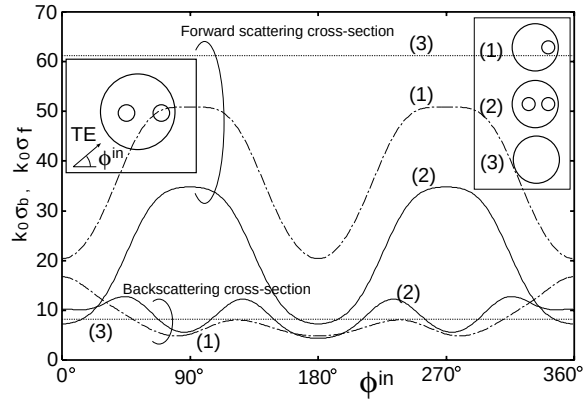

Figure 5. Backscattering cross-section $k_0\sigma_b$ and forward scattering cross-section $k_0\sigma_f$ of cylinder with a single dielectric inclusion or two dielectric inclusions for TE-wave excitation as functions of incident angle ϕ^{in}. The values of parameters are same as those given in Fig. 4.

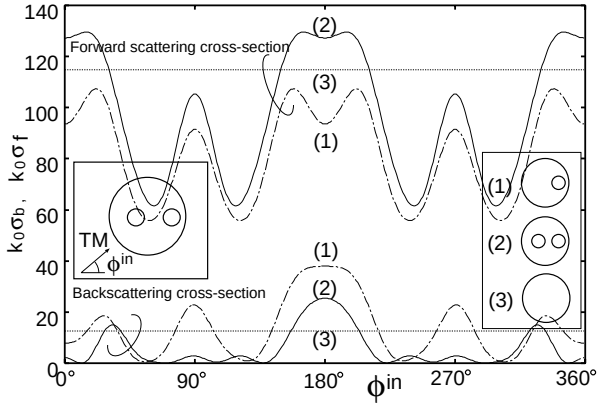

Figure 6. Backscattering cross-section $k_0\sigma_b$ and forward scattering cross-section $k_0\sigma_f$ of cylinder with a single inclusion or two inclusions of perfect conductor for TM-wave excitation as functions of incident angle ϕ^{in}, where $k_0a_1 = k_0a_2 = 0.5$, $k_0d_1 = 1.5$, $k_0d_2 = 1.0$, $\theta_1 = 0°$, $\theta_2 = 180°$, $k_0a_3 = 2.5$, and $n_3 = 2.0$. (1) a single inclusion: $|n_1| \to \infty$ and $n_2 = 2.0$, (2) two inclusions: $|n_1| = |n_2| \to \infty$, and (3) without inclusions: $n_1 = n_2 = 2.0$.

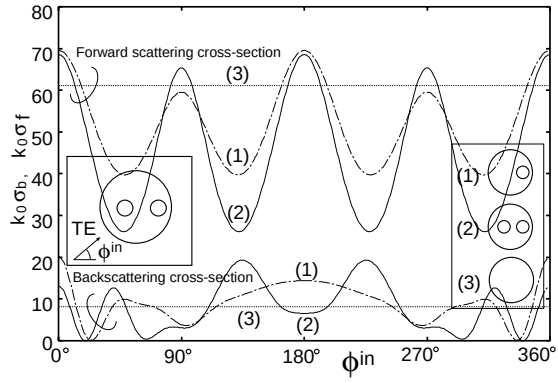

Figure 7. Backscattering cross-section $k_0\sigma_b$ and forward scattering cross-section $k_0\sigma_f$ of cylinder with a single inclusions or two inclusions of perfect conductor for TE-wave excitation as functions of incident angle ϕ^{in}. The values of parameters are same as those given in Fig. 6.

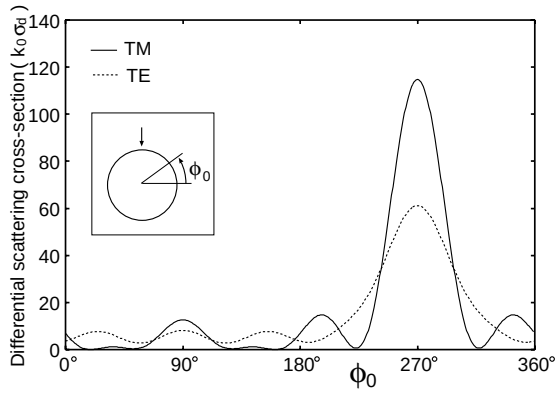

Figure 8. Differential scattering cross-section $k_0\sigma_d$ of a dielectric cylinder as functions of observation angle ϕ_0, where $k_0a_1 = 2.5$, $n_1 = 2.0$, and $\phi^{in} = 270°$.

change from those of a homogeneous host cylinder and take prominent maximums and minima at particular incident angles. These features may be used to sense the positions of internal conducting cylinders or to control the backscattering cross-section of a dielectric cylinder by embedding conducting cylinders into its inside.

We finally discuss the differential scattering cross-section $k_0\sigma_d$ of a host cylinder with three inclusions through Figs. 8 and 12 for the TM-wave and TE wave excitations. The angle of incidence

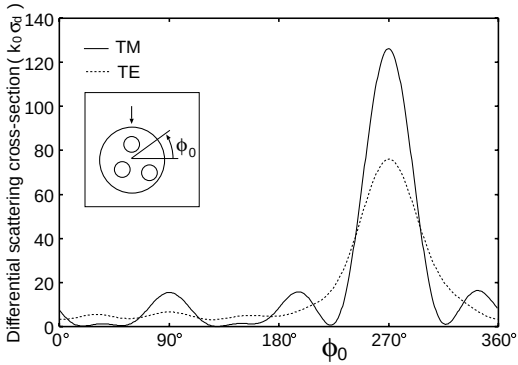

Figure 9. Differential scattering cross-section $k_0\sigma_d$ of cylinder with three inclusions of air holes as functions of observation angle ϕ_0, where $k_0a_1 = k_0a_2 = k_0a_3 = 0.3$, $n_1 = n_2 = n_3 = 1.0$, $k_0d_1 = 0.35$, $k_0d_2 = 1.0$, $k_0d_3 = 1.65$, $\theta_1 = 90°$, $\theta_2 = 210°$, $\theta_3 = 330°$, $k_0a_4 = 2.5$, $n_4 = 2.0$, and $\phi^{in} = 270°$.

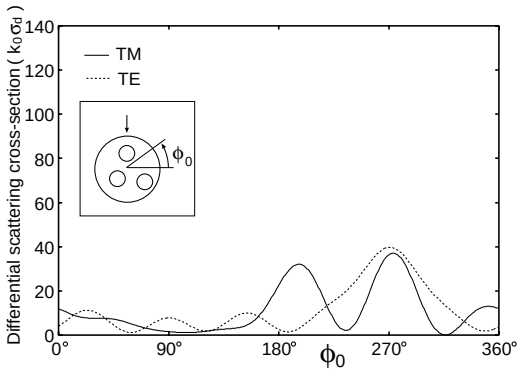

Figure 10. Differential scattering cross-section $k_0\sigma_d$ of cylinder with three dielectric inclusions as functions of observation angle ϕ_0, where $n_1 = n_2 = n_3 = 4.0$ and the values of other parameters are same as those given in Fig. 9.

is assumed to be $\phi^{in} = 270°$. The three identical cylinders with $k_0a_1 = k_0a_2 = k_0a_3 = 0.3$ are placed at the positions $k_0d_1 = 0.35$, $k_0d_2 = 1.0$, $k_0d_3 = 1.65$, $\theta_1 = 90°$, $\theta_2 = 210°$, and $\theta_3 = 330°$, respectively, in the host cylinder with $k_0a_4 = 2.5$ and $n_4 = 2.0$. The cylindrical inclusions are air holes with $n_1 = n_2 = n_3 = 1.0$ in Fig. 9, dielectric with $n_1 = n_2 = n_3 = 4.0$ in Fig. 10, perfect conductor with $|n_1| = |n_2| = |n_3| \to \infty$ in Fig. 11, and a combination of air hole

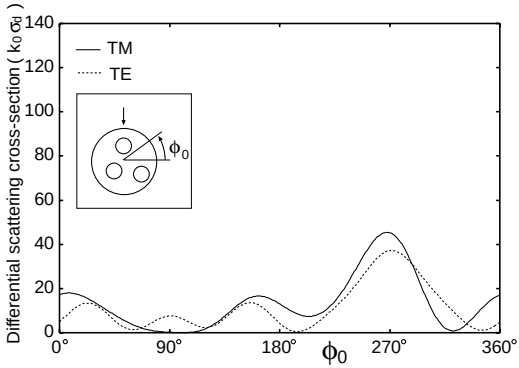

Figure 11. Differential scattering cross-section $k_0\sigma_d$ of cylinder with three inclusions of perfect conductor as functions of observation angle ϕ_0, where $|n_1| = |n_2| = |n_3| \to \infty$ and the values of other parameters are same as those given in Fig. 9.

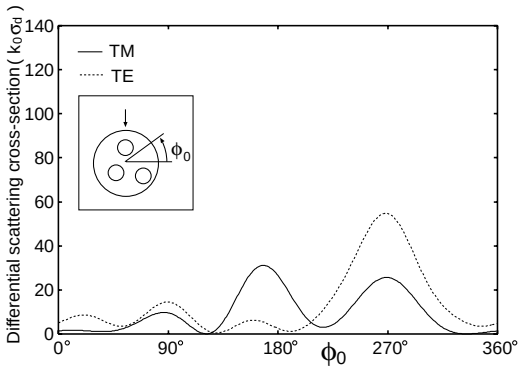

Figure 12. Differential scattering cross-section $k_0\sigma_d$ of cylinder with three inclusions of air hole, dielectric, and perfect conductor as function of angle ϕ_0, where $n_1 = 1.0$, $n_2 = 4.0$, and $|n_3| \to \infty$ and the values of other parameters are same as those given in Fig. 9.

with $n_1 = 1.0$, dielectric with $n_2 = 4.0$, and perfect conductor with $|n_3| \to \infty$ in Fig. 12, respectively. For the sake of comparison, the results for a homogeneous host cylinder without inclusions are shown in Fig. 8. The main scattering is observed in the forward direction around $\phi_0 = 270°$, though its intensity is different for TM-wave and TE-wave excitations. Regardless of polarizations, the effect of three inclusions on the differential scattering cross-section is pronounced in the forward direction. When the three inclusions are air holes (Fig. 9),

the forward scattering is enhanced with keeping the scattering in other directions mostly same as those for the homogeneous host cylinder. On the contrary, when the three inclusions are dielectric (Fig. 10), the forward scattering is strongly suppressed for both excitations and an additional scattering-lobe appears in the direction around $\phi_0 = 200^\circ$ for TM-wave excitation. If the three inclusions are perfect conductor (Fig. 11), the forward scattering is suppressed as in the case of dielectric inclusions and the scattering cross-sections for both excitations exhibit a similar profile over whole observation angle. When the three-inclusions is a combination of an air hole, a dielectric cylinder, and a conducting cylinder (Fig. 12), the forward scattering for TM-wave excitation is further suppressed and the main scattering lobe shifts in the direction around $\phi_0 = 170^\circ$, whereas the forward scattering for TE-wave excitation slightly increases compared with the case of three inclusions of dielectric (Fig. 10) and perfect conductor (Fig. 11). The comparison through Figs. 10 to 12 suggests that the TE-wave excitation is less sensitive to the inhomogeneity of internal scatterers.

4. CONCLUSIONS

A simple and direct method to analyze the two-dimensional scattering of electromagnetic plane waves from a dielectric cylinder with multiple eccentric cylindrical inclusions was presented by making use of the T-matrix approach. An aggregate T-matrix of the external cylinder with inclusions was derived for TM-wave and TE-wave excitations in terms of the T-matrices of individual cylinders isolated in the host medium. The scattered fields are easily obtained from simpler matrix calculations for the aggregate T-matrix. If the host cylinder and the inclusions have circular cross-sections, the present method is quite rigorous in the sense that the aggregate T-matrix is obtained in closed form. The only approximation involved in the analysis is a truncation of the T-matrix for numerical computations. The cylindrical inclusions may be of dielectric, air hole, perfect conductor, or their mixture.

Numerical results of the backscattering, the forward scattering and differential scattering cross-sections were presented for a circular cylinder with a single inclusion, two inclusions, and three inclusions of circular cross-sections. It was shown that the scattering characteristics have a close link to the internal asymmetry and inhomogeneity pertinent to the locations and material of cylindrical inclusions. Various numerical examples suggest that the locations of inclusions may be sensed through the backscattering cross-section and the scattering pattern of a dielectric cylinder can be effectively controlled by embedding cylindrical scatterers into its inside.

ACKNOWLEDGMENT

This work was supported in part by the 2001 Research Grant of Hoso-Bunka Foundation, Japan.

REFERENCES

1. Uzunoglu, N. K. and J. G. Fikioris, "Scattering from an infinite dielectric cylinder embedded into another," *J. Phys. A; Math. Gen.*, Vol. 12, No. 6, 825–834, 1979.
2. Kishk, A. A., R. P. Parrikar, and A. Z. Elsherbeni, "Electromagnetic scattering from an eccentric multilayered circular cylinder," *IEEE Trans. Antennas Propagat.*, Vol. AP-40, 295–303, 1992.
3. Roumeliotis, J. A., J. G. Fikioris, and G. P. Gounaris, "Electromagnetic scattering from an eccentrically coated infinite metallic cylinder," *J. Appl. Phys.*, Vol. 51, 4488–4493, 1980.
4. Parrikar, R. P., A. A. Kishk, and A. Z. Elsherbeni, "Scattering from an impedance cylinder embedded in a nonconcentric dielectric cylinder," *IEE Proc. H*, Vol. 138, 169–175, 1991.
5. Roumeliotis, J. A. and N. B. Kakogiannos, "Scattering from an infinite cylinder of small radius embedded into a dielectric one," *IEEE Trans.*, Vol. MTT-42, 463–469, 1994.
6. Stratigaki, L. G., M. P. Ioannidou, and D. P. Chrissoulidis, "Scattering from a dielectric cylinder with multiple eccentric cylindrical dielectric inclusions," *IEE Proc. Microw. Antennas Propag.*, Vol. 143, No. 6, 505–511, 1996
7. Waterman, P. C., "New formulation of acoustic scattering," *J. Acoust. Soc. Am.*, Vol. 45, 1417–1429, 1969.
8. Chew, W. C., *Waves and Fields in Inhomogeneous Media*, Sec. 8.4 and Sec. 8.6, Van Nostrand Reinhold, New York, 1990.
9. Stratton, J. A., *Electromagnetic Theory*, 374, McGraw-Hill, New York, 1941.
10. Elsherbeni, A. Z. and A. A. Kishk, "Modeling of cylindrical objects by circular dielectric or conducting cylinders," *IEEE Trans. Antennas Propagat.*, Vol. 40, No. 1, 96–99, 1992.